ХИМИЯ РАСТИТЕЛЬНОГО СЫРЬЯ. 2025. №4. С. 177–185.
KHIMIYA RASTITEL'NOGO SYR'YA, 2025, no. 4, pp. 177–185.
DOI: 10.14258/jcprm.20250416965

UDC 54-16, 67.08

PHYSICOCHEMICAL STUDY OF CEDAR BARK ETHANOL LIGNIN*

© *A.S. Kazachenko[1,2,3,4]**, Yu.N. Malyar[2,3], A.V. Levdansky[3], O.Yu. Fetisova[3], V.A. Ionin[2,3]*

[1] Reshetnev Siberian State University of Science and Technology, ave. Mira, 82, Krasnoyarsk, 660049, Russia, leo_lion_leo@mail.ru
[2] Siberian Federal University, ave. Svobodny, 79, Krasnoyarsk, 660041, Russia
[3] Institute of Chemistry and Chemical Technology, Krasnoyarsk Science Center, Siberian Branch Russian Academy of Sciences, Akademgorodok, 50/24, Krasnoyarsk, 660036, Russia
[4] Prof. V.F. Voino-Yasenetsky Krasnoyarsk State Medical University of the Ministry of Healthcare of the Russian Federation, st. Partizan Zheleznyak, bld. 1, Krasnoyarsk, Russia, 660022

This study presents the results of a comprehensive physicochemical study of ethanol lignin isolated from Siberian cedar bark performed under subcritical (190 °C, 60% ethanol) and supercritical (250 °C, 96% ethanol) processing conditions. The aim of the work was to study the effect of temperature and extraction conditions on the structural, molecular and thermal properties of lignin. The intrinsic structure properties of the isolated lignin was investigated by modern physico-chemical analysis methods, including IR spectroscopy, NMR spectroscopy, gel permeation chromatography (GPC) and thermogravimetric analysis (TGA). The registered IR-spectra revealed significant changes in the lignin structure obtained with higher processing temperature. In particular, an increase in the intensity of the absorption units associated with carboxyl groups (1706 cm^{-1}) was observed, indicating the oxidation of phenylpropane structures. The results registered by gel permeation chromatography, allowed to announce that the higher temperature of isolation leads to a shift in the molecular weight distribution towards higher molecular weights. Such results, obviously, connected with an intensification of the extraction of more complexed lignin structures. The polydispersity of the isolated samples also increases, indicating the heterogeneity of the lignin structure obtained at higher temperatures. The results of thermogravimetric analysis reveals that the main process of thermal decomposition of lignin occurs in the 150–500 °C temperature range. The ethanol lignin sample isolated at 250 °C characterized by higher thermal stability and a mass of coke residue at 700 °C in comparison to the sample isolated at 190 °C. This may be due to an increase in the molecular weight of the sample due to the condensation of fragments in the lignin structure, which makes it more resistant to thermal decomposition. The main structural units of lignin, including β-aryl ethers, pinoresinols, phenylcoumarans and guaiacyl units, were identified by 2D NMR HSQC spectroscopy. With increasing processing temperature, the destruction of β-aryl ether bonds and an increase in the number of condensed aromatic structures are observed, which confirms the condensation processes of lignin. This may be due to the homolytic decomposition of labile bonds with subsequent formation of more stable structures.

Keywords: ethanol lignin, cedar bark, FTIR, NMR, GPC.

For citing: Kazachenko A.S., Malyar Yu.N., Levdansky A.V., Fetisova O.Yu., Ionin V.A. *Khimiya Rastitel'nogo Syr'ya*, 2025, no. 4, pp. 177–185. (in Russ.). https://doi.org/10.14258/jcprm.20250416965.

Introduction

Lignin, one of the major components of plant biomass, is a complex biopolymer composed mainly by aromatic and aliphatic structures [1]. It is the second most abundant natural polymer after cellulose and plays a key role in the formation of plant cell walls, providing mechanical strength and resistance to biodegradation [2]. Due to its unique chemical structure, including aromatic rings, hydroxyl, carboxyl and methoxyl groups, lignin has a wide range of potential applications [3]. It is considered a promising raw material for the production of biopolymers, adsorbents, antioxidants, fuel additives and even carbon materials [4]. However, the effective use of lignin on an industrial scale requires a deep understanding of its underlying structural and physicochemical characteristics, which could vary significantly depending on the source of the raw material, its processing methods and extraction conditions.

* This article has electronic supplementary material (appendix), which is available to readers on the journal's website. DOI: 10.14258/jcprm.20250416965s

** Corresponding author.

The bark of coniferous trees, in particular Siberian cedar, is enriched with high-valued products. Siberian cedar is widespread in the forests of Siberia [5, 6] and is known for its high biological stability and unique chemical composition of its compounds [7]. In particular, cedar bark contains a significant amount of lignin, which could be isolated using various methods, including organosolv extraction [8]. One of these methods is organosolvent cooking in alcohols, which allows to obtain the highly pure lignin with controlled properties [9]. It is based on the application of ethanol as a solvent, which is able to effectively break the bonds between lignin and other components of plant biomass, such as cellulose and hemicellulose [10]. However, extraction conditions such as temperature, pressure and solvent concentration have a significant impact on the structure and properties of the resulting lignin [11, 12]. In this regard, studying the impact of varying of these parameters on the isolated ethanol lignin properties is an urgent aim for both scientific and practical importance.

In this work, a comprehensive study of the ethanol lignin isolated from the bark of Siberian cedar under various processing conditions was performed: in subcritical (190 °C, 60% ethanol) and supercritical (250 °C, 96% ethanol) modes. The aim of the study was to evaluate the effect of temperature and extraction conditions on the structural, molecular and thermal properties of the resulting ethanol lignin. For this purpose, modern analytical methods were used, including IR spectroscopy, NMR spectroscopy, gel permeation chromatography (GPC) and thermogravimetric analysis (TGA).

Materials and methods

The raw material used for the experiments was grinded cedar bark in a rotary knife mill RM-120 (Vibrotekhnik, St. Petersburg) with 3 mm sections of the discharge web. Moisture was removed from the grinded bark to a content of less than 1% by drying in an oven at 100–105 °C. Removal of resinous substances was accomplished by extraction with an alcohol-benzene mixture. Cedar bark ethanol lignin was obtained according to the proven method [8] with some improvements, as follows:

The process of obtaining ethanol lignin from Siberian cedar bark was carried out in a with a volume of. To the 10.0 g of Siberian cedar bark loaded into 300 ml ChemRe SYStem R-201 autoclave reactor (Korea), 100 ml of ethanol solution (60 or 96% depending on the process conditions) was added. Then, the reactor was sealed, purged with argon three times, and heated up to the desired temperature (190 or 250 °C, accordingly) under the constant stirring at 600 rpm. The organosolvent cooking was processed for 3 hours. After that, the autoclave was cooled to a room temperature, and the reaction mixture was filtered using a Buchner funnel under vacuum conditions and washed with ethanol. The obtained filtrate was further concentrated under vacuum conditions using a rotary evaporator to a volume of 50 ml and extract was cooled to a temperature of 5 °C. After that, to precipitate the ethanol lignin a five-fold volume of cooled (to 5 °C) distilled water was added. The obtained precipitate was placed in the refrigerator (at a temperature not exceeding 10 °C) for 12 hours. Finally, the precipitate was filtered using a Buchner funnel under vacuum conditions and dried at a temperature of 60 °C to a constant weight. The yield of ethanol lignin was determined by the ratio of the mass of the isolated ethanol lignin to the mass of the initial cedar bark sample. The following sample codes were assigned: EKK190 – Siberian cedar bark ethanol-lignin isolated with subcritical ethanol (60% ethanol, 190 °C); EKK250 – Siberian cedar bark ethanol-lignin isolated with supercritical ethanol (96% ethanol, 250 °C).

The FTIR spectra of ethanol lignins were recorded on an IR Fourier spectrometer IR Tracer-100 (Shimadzu, Japan) in the range of 4000–400 cm^{-1}. Samples were prepared in the form of tablets in a potassium bromide matrix under the same conditions (2 mg per 1000 mg of potassium bromide).

Thermogravimetric study and data analysis were performed using an STA 449 F1 Jupiter device (Netzsch, Germany). Thermal destruction of lignin samples was analyzed in argon in the temperature range from 30–700 °C. Heating of samples in a dynamic temperature mode (heating rate 10 °C/min) was carried out in corundum crucibles. The measurement results were processed using the Netzsch. Proteus Thermal Analysis.5.1.0 software package supplied with the device.

The weight-average molecular weight (Mw), number-average molecular weight (Mn) and polydispersity of ethanol lignin samples were determined by gel permeation chromatography using an Agilent 1260 Infinity II Multi-Detector GPC/SEC System chromatograph with triple detection: refractometer (RI), viscometer (VS) and light scattering (LS). Separation was performed on two combined columns PLgel MIXED-B and PLgel MIXED-E with a mobile phase of tetrahydrofuran (THF) stabilized with 250 ppm butylhydroxytoluene (BHT). The column was calibrated using polydisperse polystyrene standards (Agilent, USA). The eluent flow rate was 1 ml/min, the injected

sample volume was 100 μl. Before analysis, ethanol lignin samples were dissolved in the eluent with a concentration of 5 mg/ml, and then filtered through a 0.45 μm PTFE membrane filter (Millipore). Data collection and processing were performed using Agilent GPC/SEC MDS software. Molecular weights (Mn, Mw and polydispersity) were determined from calibration curves obtained using polydisperse polystyrene standards.

Two-dimensional NMR spectra were recorded at 25 °C in 5 mm ampoules on a Bruker AVANCE III 600 spectrometer operating at 600 MHz (1H) and 150 MHz (13C). About 80 mg of sample was dissolved in 0.6 ml of deuterated dimethyl sulfoxide, then the spectra were recorded in HSQC (Heteronuclear Single Quantum Correlation) experiments with editing (HSQCed) from the Bruker standard sequence library. The solvent signal (δC 40.1; δH 2.5) was used as an internal standard.

Results and discussion

A native-like lignin commonly named Brauns` lignin is traditionally isolated from plant biomass under relatively mild conditions: extraction processing performed at room temperature in neutral alcoholic solvents [13, 14]. Alongside the apparent preservation of ethanol lignin's` natural characteristics such method is accompanied by few disadvantages: low yields of targeted substance, its contamination with carbohydrates and enzymes and changes if the polymer structure (both depolymerization and condensation). At the same time, the performed organosolvent cooking of cedar bark under sub- and supercritical conditions allows us to decompose the up mentioned byproducts of extraction, which results in the maximum yields of ethanol lignin and its high degree of purity.

To confirm the results, ethanol lignin samples isolated under different conditions were analyzed by FTIR, NMR spectroscopy, gel permeation chromatography and thermal analysis.

The IR spectra of the ethanol lignin samples isolated under sub- and supercritical ethanol conditions, characterized by the following similarities and differences in absorbance units (a.u.).

According FTIR analysis intense a.u. with an increased width observed in the 3400 cm^{-1} region, mainly associated with the stretching vibrations of hydroxyl groups linked by hydrogen bonds [15], are common for both samples. This indicates that the resulting products characterized by high content of free hydroxyl groups, which possibly could be used for chemical modification processes.

The combined a.u. presence in 3000–2800 and 1470–1450 cm^{-1} regions are attributed to the stretching and deformation vibrations of C-H in methyl and methylene groups [16, 17]. Also, the triplet of a.u. with maxima at 1605, 1510, and 1455 cm^{-1} could be connected with the C=C bonds vibrations, which are the aromatic rings [18]. Still, depending on the isolation condition used, these a.u. undergo a rearrangement and slightly shifted to the low-frequency region in case of EKK190. Moreover, an a.u. at 1605 could be connected with sorbed water. The similar rearrangement of a.u. at 1365 and 1380 cm^{-1} corresponding to the vibrations of $C(CH_3)$ groups, is observed for both of samples, which are also typical for guaiacylsyringyl-type lignin [16]. The observed a.u. at 760 cm^{-1} region are attributed to vibrations of the $(CH_2)_4$ skeleton, and differs for both samples insignificantly.

Thus, the most important difference, in course of the present study, could be observed in a noticeable increase in the integral intensity of the a.u., registered at 1705 and at 1605 cm^{-1}. These a.u. corresponds to vibrations of carboxyl groups (reaching its highest intensity for EKK250), and vibrations of aromatic rings (reaching its highest intensity for EKK190), accordingly. This fact, obviously, indicates an increase in the number of carboxyl groups due to the side chains` oxidation during the isolation.

The thermogravimetry (TG) and differential thermogravimetric (DTG) analysis are widely used to study thermal transformations of plant biopolymers, which make it possible to evaluate the stability of a substance in certain temperature ranges and obtain quantitative characteristics of pyrolysis [19, 20]. The lignins under study do not differ fundamentally in the nature of thermolysis in an inert environment. Figures 1 and 2 show the TG/DTG profiles of thermal destruction of ethanol lignins. It is evident that the DTG decomposition curves are similar to each other and represent broad peaks characteristic of lignins.

Thermal decomposition occurs in three stages. Up to a temperature of 200 °C, the mass loss of samples EKK190 and EKK250 is 2 and 3%, respectively. This period is characterized by the loss of water. The large range of water desorption can be explained by the difficulty of breaking the hydrogen bonds between water molecules and the polar functional groups of lignin [21].

The main thermal decomposition of all the studied lignins occurs in the range of 150–500 °C. The difference lies only in the rate of mass loss of the samples and the temperature at which this rate is maximum. In this period, the samples lose half of their initial mass (Table 1). During the main thermal decomposition, the maximum mass

loss was observed for sample EKK190, which may indirectly indicate the presence of a smaller number of thermally stable fractions in its structure compared to the original ethanol lignin, which are subject to decomposition in the specified range. At higher temperatures, the formation of coke residue begins due to the condensation of the lignin structure. According to [22], in the temperature range of 230–260 °C, degradation of the propane side chains of lignin occurs, with the formation of methyl, ethyl and vinyl derivatives of guaiacol. In addition, at temperatures ≤310 °C, ether bonds, which have low thermal stability, are subject to destruction [23]. At temperatures above 400 °C, the structure of the products formed in the previous stage begins to change due to the rupture of bonds and the volatilization of groups involved in the condensation and reorganization processes, leading to the formation of products with a high carbon content. This stage of carbonization is accompanied by a small and gradual loss of mass, which can be observed on the TG graph (Fig. 1). In addition, the evaporating compounds undergo secondary thermolytic reactions in the gas phase, which do not affect the mass of the remaining sample.

At the end of thermolysis (700 °C), sample EKK190 shows minimal coked residue, which also indirectly indicates minimal heat resistance of the sample. EKK190 has a number-average molecular weight (Mn) of 412, a weight-average molecular weight (Mw) of 461 and polydispersity (PD) of 3.55. According to the MWD data (Fig. 3), sample EKK190 is characterized by a monomodal distribution with a small shoulder in the region of 200 Da, which can be attributed to mono- and dimers of phenylpropane derivatives. Compared with ethanol lignins of coniferous wood [24, 25], the obtained samples are characterized by a wider MWD, probably due to the heterogeneity of the bark and the extraction of not only lignin, but also other components.

An increase in the temperature of cedar bark processing leads to a change in the MWD profile of the obtained lignin. Thus, a shift to the region of higher molecular weights is observed, which indicates an intensification of the process of extraction of lignin molecules with a change in the process conditions. The nature of the MWD remains the same - monomodal, and the shoulder in the 200 Da region is also preserved. At the same time, the number of "heavier" molecules increases, which leads to an increase in the average number and average weight molecular weights to 605 and 2519 Da, respectively (Table 2). Due to the presence of new fractions, polydispersity also increases – to 4.16. It is worth noting that both samples contain low-molecular components with a mass in the range of 50–150 Da. Probably, these are unextracted components of the resinous substances of cedar bark - monoterpenoids, including α-pinene, Δ3-carene, β-phellandrene and others.

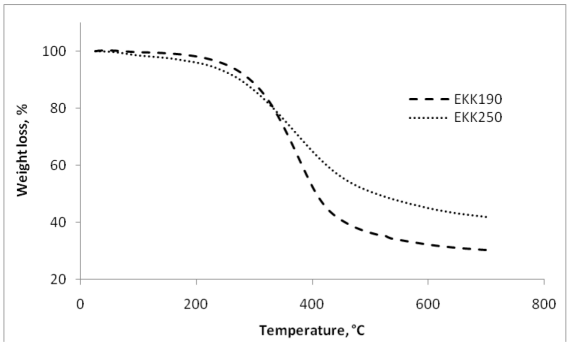

Fig. 1. Result of thermogravimetric analysis (TG) of samples

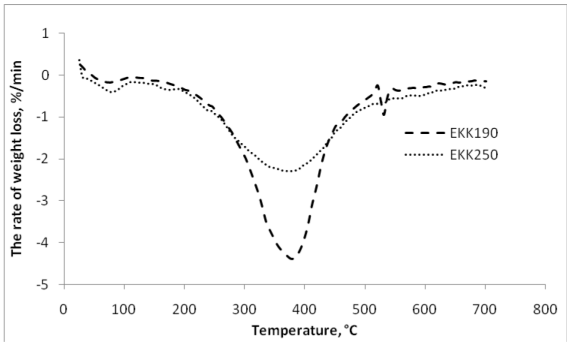

Fig. 2. Result of differential thermogravimetric analysis (DTG) of samples

Table 1. Thermogravimetric characteristics

Sample	Main decomposition, °C Weight loss, %	T_{max} °C V_{max}, %/min	Remainder at 700 °C, %
EKK190	155–500 62.8	378 4.3	30.4
EKK250	154–500 46.8	375 2.3	41.9

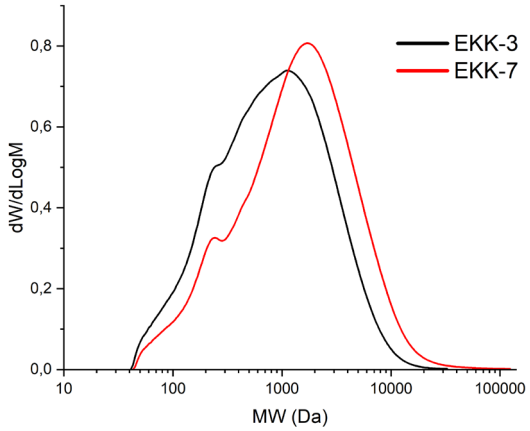

Fig. 3. Gel permeation chromatograms of cedar bark ethanol lignin samples obtained under different conditions

Table 2. Molecular weight characteristics of cedar bark ethanol lignins

Sample	Mn (Da)	Mw(Da)	PD
EKK190	412	1461	3.55
EKK250	605	2519	4.16

The structure of the EKK190 and EKK250 samples isolated from cedar bark was studied using 2D HSQC NMR spectroscopy. Their 2D HSQC NMR spectra consist of three main regions: aliphatic oxygenated (oxygen-containing) (δC/δH 90–50/5.7–2.9) (Fig. 4), aromatic (δC/δH 150–100/8.0–5.5) (Fig. 1 is presented in the electronic supplemental material) and aliphatic non-oxygenated (δC/δH 50–0/3.0–0.5) (Fig. 2 is presented in the electronic supplemental material). The aliphatic oxygenated region mainly contains correlation signals of lignin side chain atoms, the aromatic region contains signals of aromatic rings, and the aliphatic non-oxygenated region contains signals of saturated acyclic structures. The assignment of the main ^{1}H-^{13}C peaks in the HSQC spectra was performed using literature data [26–28] and is given in Table 2.

The table also shows the chemical shift values of some of the low-intensity peaks, the images of which are missing in Figures 4 and Figures 1, 2 is presented in the electronic supplemental material. The main structural units and fragments of the samples are shown in Figure 5. Comparison of the region of side chain signals of ^{1}H-^{13}C HSQC spectra of EKK190 and EKK250 (Fig. 4) showed that the EKK190 sample contains correlation peaks of β-aryl ethers (A), pinoresinol (B) and phenylcoumarane fragments (C) of lignin (Fig. 5). Some of the β-aryl ethers are ethoxylated at the α-position, since the spectrum contains signals of the methylene group in the α-ethoxylated β-O-4′ bonds (δC/δH 63.8/3.33) and the α-position of the α-acylated β-O-4′ bonds (δC/δH 79.9/4.50). In addition, in this region of the spectrum, a signal of the Cγ-Hγ correlations of the terminal groups of cinnamyl alcohol (I) and a high-intensity signal in the region of δC/δH 56.5/3.45 ppm, assigned to the CH_2 group of residual ethanol, were detected. In the considered region of the spectrum of the EKK250 sample, the absence of most of the signals of β-aryl ethers (A), α-ethoxylated β-aryl ethers (A′) of pinoresinol (B) and phenylcoumarane fragments (C) of lignin is observed. The cleavage of the β-O-4′, β-β′, β-5′ bonds between the monomer units of lignin is probably explained by the higher temperature (250 °C) of obtaining this sample. This conclusion is indirectly confirmed by a significant increase in the intensity of the Cγ-Hγ correlation signal of the terminal groups of cinnamyl alcohol (I) at δC/δH 60.1/4.03 ppm.

The aromatic region of ^{1}H-^{13}C HSQC spectra of samples EKK190 and EKK250 (Fig. 1 is presented in the electronic supplemental material) contains characteristic correlation peaks of guaiacyl units (G), p-coumarates (pCA), and stilbenes (St). Interestingly, within its boundaries, sample EKK250 is distinguished by high intensity of signals at δC/δH 120.5/6.58 and 112.5/6.76 ppm, typical for correlations of C6-H6 and C2-H2 5-5′ condensed subunits (L) [29, 30]. Whereas in sample EKK190, on the contrary, these signals have a rather weak intensity. At the same time, the intensity of the signals of C6-H6 and C2-H2 guaiacyl units (G) in sample EKK190 remains high, and in sample EKK250 it decreases noticeably. According to a number of authors [26], the formation of 5-5' condensed structures with increasing temperature of organosolvent extraction occurs as a result of homolytic cleavage of some labile β-O-4' bonds and subsequent reactions of repeated radical binding. The aliphatic non-oxygenated region of the HSQC spectra of samples EKK190 and EKK250 is represented by fairly intense signals of saturated hydrocarbon fragments. Some of them probably belong to extractive substances (e.g. residues of saturated fatty acids), and some to difficult to identify

lignin degradation products [31]. Thus, two clear peaks at δC/δH 24.8/1.51 and δC/δH 14.2–14.4/0.84–0.86 ppm, most likely, belong to the Cβ-Hβ and Cγ-Hγ correlations of the terminal groups of 4-n-propyl (P), formed as a result of the cleavage of the β-O-4′ bond [32, 33]. No fundamental differences were found between the samples in this region, with the exception of the presence in the EKK190 sample of two high-intensity correlation signals (δC/δH 19.1/1.04 and 31.2/2.10 ppm), attributed to the CH_3 groups of residual ethanol and acetone, respectively.

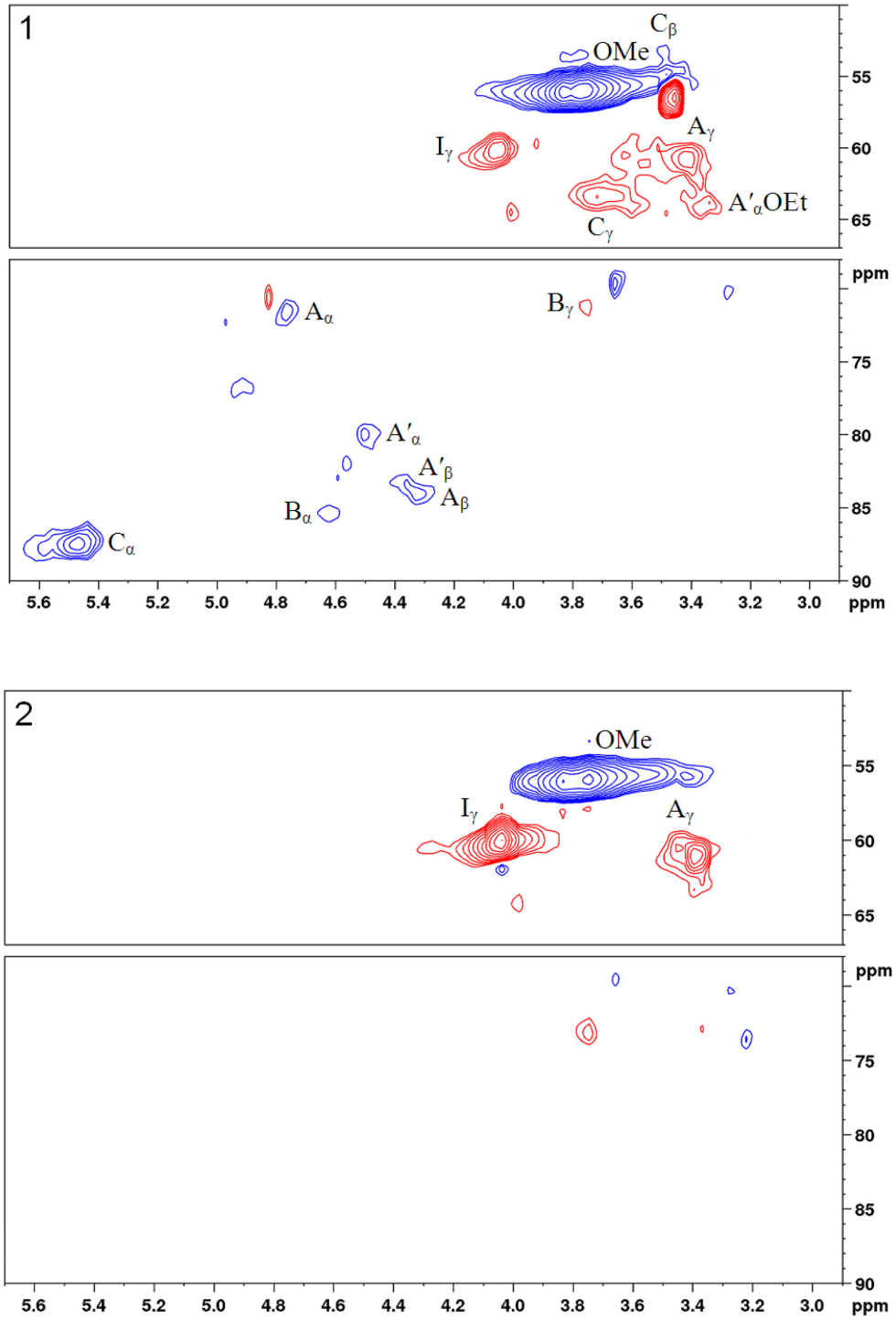

Fig. 4. Aliphatic oxygenated regions in HSQCed spectra of EKK-190 (1) and EKK-250 (2) samples. The assignment of signals is given in Table 3 and the main identified structural units and fragments are shown in Fig. 5

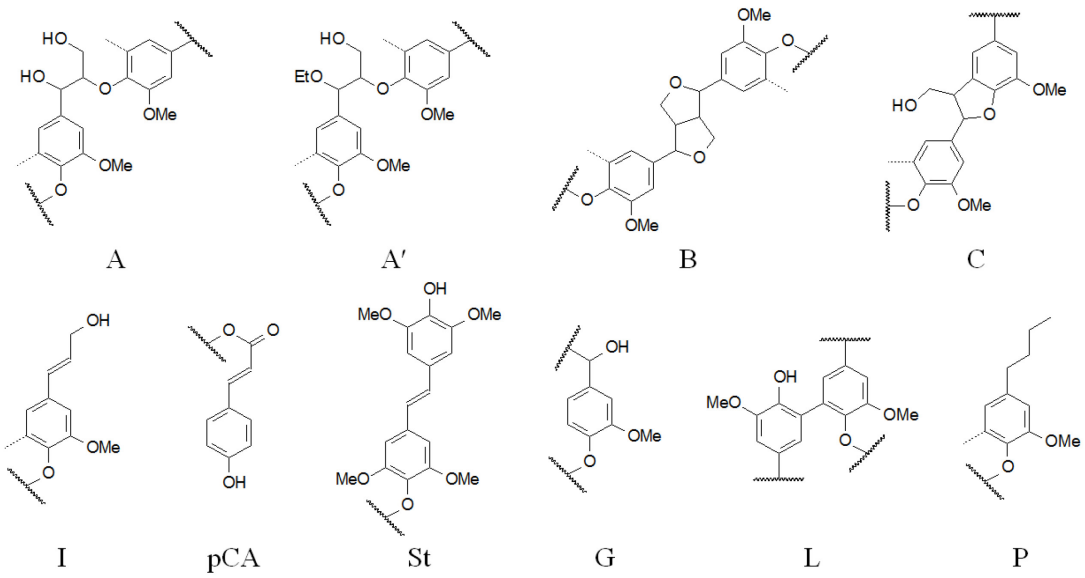

Fig. 5. Main structure units and fragments of EKK-190 and EKK-250 samples: A – β-aryl ethers, A′ – α-ethoxylated (C_αOEt) β-aryl ethers, B – pinoresinols, C – phenylcoumarans, I – cinnamyl alcohol end groups, pCA – p-coumarates, St – stilbenes, G – guaiacyl units, L – 5-5’ condensed subunits, P – 4-*n*-propyl end groups

Table 3. Assignments of the ^{1}H-^{13}C cross signals in the HSQC spectra of EKK-190 and EKK-250 samples

Lable	δ_C/δ_H, ppm (EKK-190)	δ_C/δ_H, ppm (EKK-250)	Assignments
OMe	56.0/3.77	55.9/3.74	C-H in methoxyls (OMe)
A_γ and A'_γ	60.7/3.42−3.62	60.5/3.45	C_γ-H_γ in β-aryl ether (β-O-4′) substructures (A) and in α-ethoxylated (C_αOEt) β-aryl ether (β-O-4′) substructures (A′)
A_β and A'_β	84.0/4.32 and 83.4/4.36	–	C_β-H_β in β-aryl ether (β-O-4′) substructures (A) and in α-ethoxylated (C_αOEt) β-aryl ether (β-O-4′) substructures (A′)
A_α	71.5/4.77	–	C_α-H_α in β-aryl ether (β-O-4′) substructures (A)
A'_αOEt	63.9/3.33	–	C-H of methylene group in α-ethoxylated (C_αOEt) β-aryl ether (β-O-4′) substructures (A′)
A'_α	79.9/4.50	–	C_α-H_α in α-ethoxylated (C_αOEt) β-aryl ether (β-O-4′) substructures (A′)
B_β	54.2/3.09	–	C_β-H_β in pinoresinol (β-β′) substructures (B)
B_γ	71.3/3.74 and 4.15	–	C_γ-H_γ in pinoresinol (β-β′) substructures (B)
B_α	85.4/4.62	–	C_α-H_α in pinoresinol (β-β′) substructures (B)
C_β	53.3/3.48	–	C_β-H_β in phenylcoumaran (β–5′) substructures (C)
C_γ	63.4/3.71	–	C_γ-H_γ in phenylcoumaran (β-5′) substructures (C)
C_α	87.5/5.47	–	C_α-H_α in phenylcoumaran (β-5′) substructures (C_α)
I_γ	60.2/4.06	60.1/4.03	C_γ-H_γ in cinnamyl alcohol end groups (I)
$pCA_{3,5}$	115.7/6.76	116.1/6.76	$C_{3,5}$-$H_{3,5}$ in p-coumarate (pCA)
$pCA_{2,6}$	128.4/7.41	128.0/7.41	$C_{2,6}$-$H_{2,6}$ in p-coumarate (pCA)
G_2	111.1/6.94	110.4/6.97	C_2-H_2 in guaiacyl units (G)
L_2	113.2/6.76	112.5/6.76	C_2-H_2 in 5-5′ condensed subunits (L)
G_5	115.6/6.70 and 115.7/6.94	115.7/6.68 and 116.1/6.92	C_5-H_5 in guaiacyl units (G)
G_6	118.7/6.79	119.1/6.76	C_6-H_6 в in guaiacyl units (G)
L_6	120.7/6.56	120.5/6.58	C_6-H_6 in 5-5′ condensed subunits (L)
St_2	109./7.15	109.7/7.14	C_2-H_2 in stilbenes (St)
$St_{\alpha,\beta}$	126.2/6.97	126.0/6.97	$C_{\alpha,\beta}$-$H_{\alpha,\beta}$ in stilbenes (St)
P_β	24.8/1.51	24.8/1.51	C_β-H_β in 4-*n*-propyl end groups (P)
P_γ	14.4/0.86	14.2/0.84	C_γ-H_γ in 4-*n*-propyl end groups (P)

Conclusions

Increasing the cedar bark processing temperature from 190 °C to 250 °C leads to significant changes in the ethanol lignin structure. In particular, the destruction of β-aryl ether bonds and an increase in the content of carboxyl groups are observed, which is confirmed by IR and NMR spectroscopy data. Gel permeation chromatography showed that an increase in the processing temperature leads to a shift in the molecular weight distribution towards higher molecular weights, which indicates an intensification of the lignin extraction process. The polydispersity of the samples also increases, indicating a heterogeneity of the lignin structure. Thermogravimetric analysis revealed that the main process of thermal decomposition of lignin occurs in the range of 150–500 °C. The sample obtained at 250 °C demonstrates higher thermal stability and a larger residue at 700 °C compared to the sample obtained at 190 °C. The main structural units of lignin, including β-aryl ethers, pinoresinols, phenylcoumarans and guaiacyl units, were identified using 2D NMR HSQC spectroscopy. With increasing processing temperature, an increase in the number of condensed aromatic structures is observed, indicating lignin condensation processes.

The data obtained could be used in perspective for optimizing the processes of lignin isolation from cedar bark with its further application as a raw material for the production of biopolymers [34] and other materials with modified properties [35, 36].

Supplementary Information
The electronic supplement to the article (DOI: http://www.doi.org/10.14258/jcprm.20250416965s) provides additionalexperimental material that reveals the main points set out in the article

Funding
This study was carried out within the budget plan FWES № 0287-2021-0017 for the Institute of Chemistry and Chemical Technology, Siberian Branch of the Russian Academy of Sciences, on the equipment of the Krasnoyarsk Regional Center for Collective Use, Krasnoyarsk Science Center.

Conflict of Interest
The authors of this work declare that they have no conflicts of interest.

Open Access
This article is distributed under the terms of the Creative Commons Attribution 4.0 International License (https://creativecommons.org/licenses/by/4.0/), which permits unrestricted use, distribution, and distribution in any medium provided you give appropriate credit to the original author(s) and the source and link to the Creative Commons license, and indicate if they were modified.

References

1. Zhang Y., Naebe M. *ACS Sustainable Chemistry & Engineering*, 2021, vol. 9, no. 4, pp. 1427–1442. https://doi.org/10.1021/acssuschemeng.0c06998.
2. Karmanov A.P., Ermakova A.V., Raskosha O.V. et al. *Russian Journal of Bioorganic Chemistry*, 2024, vol. 50, pp. 2657–2674. https://doi.org/10.1134/S106816202407001X.
3. Fabbri F., Bischof S., Mayr S., Gritsch S., Jimenez Bartolome M., Schwaiger N., Guebitz G.M., Weiss R. *Polymers*, 2023, vol. 15, no. 7, 1694. https://doi.org/10.3390/polym15071694.
4. Yu O., Kim K.H. *Applied Sciences*, 2020, vol. 10, no. 13, 4626. https://doi.org/10.3390/app10134626.
5. Wang Q.-Y., Jia H.-B., Shang J. *Journal of Forestry Research*, 2005, vol. 16, no. 2, pp. 93–96.
6. Stashkevich N.Yu. *Forestry Journal*, 2015, no. 3, pp. 35–42.
7. Tiina A., Lantto H.J., Dorman D., Shikov A.N., Pozharitskaya O.N., Makarov V.G., Tikhonov V.P., Hiltunen R., Raasmaja A. *Food Chemistry*, 2009, vol. 112, no. 4, pp. 936–943.
8. Ionin V.A., Kazachenko A.S., Elsufiev E.V. *Bulletin of Tomsk State University. Chemistry*, 2021, no. 23.
9. Quesada-Medina J., Cremades F., Olivares Carrillo P. *Bioresource Technology*, 2010, vol. 101, pp. 8252–8260.
10. Zijlstra D.S., Lahive C.W., Analbers C.A., Figueirêdo M.B., Wang Z., Lancefield C.S., Deuss P.J. *ACS Sustainable Chemistry & Engineering*, 2020, vol. 8, no. 13, pp. 5119–5131. https://doi.org/10.1021/acssuschemeng.9b07222.
11. Zijlstra D.S., Analbers C.A., de Korte J., Wilbers E., Deuss P.J. *Polymers*, 2019, vol. 11, no. 12, 1913. https://doi.org/10.3390/polym11121913.
12. Bergrath J., Rumpf J., Burger R., Do X.T., Wirtz M., Schulze M. Macromolecular Materials and Engineering, 2023, vol. 308, no. 8, 2300093. https://doi.org/10.1002/mame.202300093.
13. Hiltunen E., Alvila L., Pakkanen T. *Wood Science and Technology*, 2006, vol. 40, pp. 575–584.
14. Wang Z., Deuss P.J. *Biotechnology Advances*, 2023, vol. 68, 108230.
15. Iqbal D.D., Nazir A., Iqbal M. et al. *Green Processing and Synthesis*, 2020, vol. 9, pp. 212–218.
16. Golubkov V., Borovkova V., Lutoshkin M. et al. *Wood Science and Technology*, 2024, vol. 58, pp. 1861–1879.
17. Sammons R.J., Harper D.P., Labbé N., Bozell J.J., Elder T., Rials T.G. *BioResources*, 2013, vol. 8, no. 2, pp. 2752–2767.

18. Larkin P. *Infrared and Raman Spectroscopy; Principles and Spectral Interpretation*. Elsevier, 2011.
19. Nurazzi N.M., Asyraf M.R.M., Rayung M., Norrrahim M.N.F., Shazleen S.S., Rani M.S.A., Shafi A.R., Aisyah H.A., Radzi M.H.M., Sabaruddin F.A. et al. *Polymers*, 2021, vol. 13, no. 16, 2710. https://doi.org/10.3390/polym13162710.
20. Fetisova O.Y., Mikova N.M., Chesnokov N.V. *Kinetics and Catalysis*, 2019, vol. 60, pp. 273–280. https://doi.org/10.1134/S0023158419030054.
21. Osovskaya I.I. et al. [*Khitin-glyukanovyye kompleksy. Fiziko-khimicheskiye svoystva i molekulyarnyye kharakteristiki. Uchebnoye posobiye. Chitin-glucan complexes. Physicochemical properties and molecular characteristics. Study guide*]. St. Petersburg, 2010, 52 p. (in Russ.).
22. Hansen B., Kusch P., Schulze M., Kamm B. *Journal of Polymers and the Environment*, 2016, vol. 24, no. 2, pp. 85–97. https://doi.org/10.1007/s10924-015-0746-3.
23. Wittkowski R., Ruther J., Drinda H., Rafiei-Taghanaki F. *Formation of smoke flavor compounds by thermal lignin degradation*. ACS symposium series, Washington, DC, 1992, pp. 232–490. https://doi.org/10.1021/BK-1992-0490.CH018.
24. Borovkova V.S., Malyar Y.N., Vasilieva N.Y., Skripnikov A.M., Ionin V.A., Sychev V.V., Golubkov V.A., Taran O.P. *Materials*, 2023, vol. 16, no. 4, 1525. https://doi.org/10.3390/ma16041525.
25. Malyar Yu.N., Sharypov V.I., Kazachenko A.S., Levdansky A.V. *Journal of Siberian Federal University. Chemistry*, 2019, vol. 12, no. 1, pp. 73–86. https://doi.org/10.17516/1998-2836-0109. (in Russ.).
26. You T.-T., Mao J.-Z., Yuan T.-Q., Wen J.-L., Xu F. *Journal of Agricultural and Food Chemistry*, 2013, vol. 61, no. 22, pp. 5361–5370. https://doi.org/10.1021/jf401277v.
27. Wen J.-L., Sun S.-L., Yuan T.-Q., Xu F., Sun R.-C. *Journal of Agricultural and Food Chemistry*, 2013, vol. 61, no. 46, pp. 11067–11075. https://doi.org/10.1021/jf403717q.
28. Bauer S., Sorek H., Mitchell V.D., Ibáñez A.B., Wemmer D.E. *Journal of Agricultural and Food Chemistry*, 2012, vol. 60, no. 33, pp. 8203–8212. https://doi.org/10.1021/jf302409d.
29. Rietzler B., Karlsson M., Kwan I., Lawoko M., Ek M. *Biomacromolecules*, 2022, vol. 23, no. 8, pp. 3349–3358. https://doi.org/10.1021/acs.biomac.2c00457.
30. Karlsson M., Giummarella N., Lindén P.A., Lawoko M. *ChemSusChem*, 2020, vol. 13, no. 17, pp. 4666–4677. https://doi.org/10.1002/cssc.202000974.
31. Eugenio M.E., Martín-Sampedro R., Santos J.I., Wicklein B., Ibarra D. *Molecules*, 2021, vol. 26, no. 13, 3819. https://doi.org/10.3390/molecules26133819.
32. Smit A.T., Dezaire T., Riddell L.A., Bruijnincx P.C.A. *ACS Sustainable Chemistry & Engineering*, 2023, vol. 11, no. 15, pp. 6070–6080. https://doi.org/10.1021/acssuschemeng.3c00617.
33. Wang S., Gao W., Xiao L.-P., Shi J., Sun R.-C., Song G. *Sustainable Energy & Fuels*, 2019, vol. 3, no. 2, pp. 401–408. https://doi.org/10.1039/C8SE00359A.
34. Kuznetsov B.N., Vasilyeva N.Y., Kazachenko A.S. et al. *Wood Science and Technology*, 2020, vol. 54, pp. 365–381. https://doi.org/10.1007/s00226-020-01157-6.
35. Vasile C., Baican M. *Polymers*, 2023, vol. 15, no. 15, 3177. https://doi.org/10.3390/polym15153177.
36. Taran O.P., Miroshnikova A.V., Baryshnikov S.V., Kazachenko A.S., Skripnikov A.M., Sychev V.V., Malyar Y.N., Kuznetsov B.N. *Catalysts*, 2022, vol. 12, no. 11, 1384. https://doi.org/10.3390/catal12111384.

Received March 7, 2025

Revised October 23, 2025

Accepted November 30, 2025

Information about authors

Kazachenko Alexander Sergeevich – Candidate of Chemical Sciences, Associate Professor of Fundamental Chemistry Department, leo_lion_leo@mail.ru

Maliar Yuri Nikolaevich – Candidate of Chemical Sciences, Senior Researcher, yumalyar@gmail.com

Levdansky Alexandr Vladimirovich – Candidate of Chemical Sciences, Researcher, alexsander.l@mail.ru

Fetisova Olga Yurievna – Candidate of Chemical Sciences, Researcher, fou1978@mail.ru

Ionin Vladislav Alexandrovich – Junior Researcher, ionin.va@icct.krasn.ru